Modelling metastatic melanoma in zebrafish

Groenewoud, A.

Chapter 3:

Evaluation of (*fli:GFP*) x *Casper* Zebrafish Embryos as a Model for Human Conjunctival Melanoma

Chapter 3: Evaluation of (fli:GFP) Casper Zebrafish Embryos as a Model for Human Conjunctival Melanoma

Kelly Cristine de Sousa Pontes[*]; Arwin Groenewoud[†]; Jinfeng Cao[*]; Livia Maria Silva Ataide[+]; Ewa Snaar-Jagalska[†±]; Martine J. Jager*[±]

Author Affiliations & Notes

*Department of Ophthalmology, Leiden University Medical Center, Leiden, The Netherlands

[†]Institute of Biology, Leiden University, Leiden, The Netherlands

[+]Department of Population Biology, Institute for Biodiversity and Ecosystem Dynamics, University of Amsterdam, Amsterdam, The Netherlands

†Institute of Biology, Leiden University, Leiden, The Netherlands

*Martine J. Jager

Correspondence: Martine J. Jager, Department of Ophthalmology, Leiden University Medical Center, P.O. Box 9600, 2300 RC Leiden, The Netherlands; m.j.jager@lumc.nl.

Footnotes: [±] ES-J and MJJ contributed equally to the work presented here and should therefore be regarded as equivalent authors.

Published as: *Kelly Cristine de Sousa Pontes*; Arwin Groenewoud†; Jinfeng Cao*; Livia Maria Silva Ataide+; Ewa Snaar-Jagalska†±; Martine J. Jager*±*
Evaluation of (fli:GFP) Casper Zebrafish Embryos as a Model for Human Conjunctival Melanoma
Investigative Ophthalmology & Visual Science December 2017, Vol.58, 6065-6071. doi:https://doi.org/10.1167/iovs.17-22023

Abstract

Purpose: Conjunctival melanoma (CM) is a rare malignant disease that can lead to recurrences and metastases. There is a lack of effective treatments for the metastases, and we set out to develop a new animal model to test potential therapies. Zebrafish are being used as a model for many diseases, and our goal was to test whether this animal could be used to study CM.

Methods: Three human CM cell lines (CRMM-1 and CM2005.1, which both harbor a *B-RAF* mutation, and CRMM-2, which has an *N-RAS* mutation) were injected into the yolk sac, around the eye, and into the duct of Cuvier of transgenic (*fli:GFP*) *Casper* zebrafish embryos. Fluorescent and confocal images were taken to assess the phenotype and the behavior of engrafted cells and to test the effect of Vemurafenib as a treatment against CM.

Results: While the cells that had been injected inside the yolk sac died and those injected around the eye sporadically went into the circulation, the cells that had been injected into the duct of Cuvier colonized the zebrafish: cells from all three cell lines proliferated and disseminated to the eyes, where they formed clusters, and to the tail, where we noticed extravasation and micro-metastases. Vemurafenib, a potent agent for treatment of B-RAF V600E–positive melanoma, inhibited outgrowth of CRMM-1 and CM2005.1 cells in a mutation-dependent way.

Conclusions: The (*fli:GFP*) *Casper* zebrafish embryo can be used as an efficient animal model to study metastatic behavior of human CM cells and warrants further testing of drug efficacy to aid care of CM patients.

Introduction

Conjunctival melanoma (CM) is a rare malignant ocular disease, accounting for 5% to 10% of all human ocular melanoma[1]. Over the past decades, its incidence has increased worldwide[2–4]. The current treatment of choice for primary CM is wide surgical excision, combined with brachytherapy, cryotherapy, and topical chemotherapy (e.g., mitomycin C). However, effective targeted therapies have not yet been developed to treat this malignancy[5]; CM's high recurrence rate is associated with metastasis and poor prognosis[6–8]. Furthermore, the mortality rate is high, ranging from 13% to 38% after 10 years[9–11].

In this malignancy, essential mutations occur in the *B-RAF* and *N-RAS* genes[5,12–14]. *B-RAF* mutations constitutively activate the mitogen-activated protein kinase (MAPK) pathway and its downstream kinases MEK1/2-ERK1/2, promoting tumor proliferation[15,16].

Mice have previously been used as a model to study human CM,[17,18] but there are some limitations. The major disadvantages are a slow growth and spread of the tumor, which can take weeks to months, and the high cost for reproduction and housing. The cost increases further when immunosuppressive drugs are needed to prevent tumor rejection[19]. Therefore, there is a need to find a new animal model.

The zebrafish model has been used widely in research because of its advantages, such as (1) the fish's high fecundity and short time between generations, (2) the high interspecies conservation of molecular pathways between zebrafish and mammals,[20–22] (3) their transparency, allowing direct imaging of development, organogenesis, and cancer progression,[23] which enables tracking of transplanted cells,[24] (4) the possibility of xenotransplantation, and (5) their permeability to small molecular weight compounds from water, enabling easy delivery and efficient screening of large numbers of anticancer compounds[19].Furthermore, the fact that their adaptive immune system does not reach maturity until 4-weeks postfertilization allows them to be used without the need for immunosuppression in the embryonic stages[20].

There are no studies showing whether zebrafish embryos can be used as an animal model for human CM, and our goal was to determine if this animal can be used as a screening platform based on the xenotransplantation of three human CM cell lines. Our group has shown that two of three available CM cell lines, CRMM1[25] and CM2005.1,[26] harbor a *B-RAF V600E* mutation, while the third, CRMM2, contains an *N-RAS Q61L* mutation[17,27]. We injected stable red fluorescently labeled (lentiviral

tdTomato-blas) CM cells via different routes into the embryonic zebrafish. Thus, we determined the most effective engraftment strategy for the establishment of CM xenograft tumors in zebrafish and we observed distinct phenotypes after implantation of the three CM cell lines. We subsequently validated the model through the use of the well-known B-RAF inhibitor, vemurafenib.

Material and Methods

Cell Culture

We used three CM cell lines, CRMM-1, CRMM-2, and CM2005.1, all generated from recurrent primary CM. The CRMM-1 and CRMM-2 cell lines, isolated by Nareyeck et al.,[25] were cultured in F-12K nutrient mixture, Kaighn's modification (Gibco, Life Technologies, Bleiswijk, The Netherlands), supplemented with 10% heat-inactivated fetal bovine serum (FBS; Greiner Bio-one, Alphen aan den Rijn, The Netherlands) and 1% Penicillin/Streptomycin (Gibco). CM2005.1, established in 2007 by Keijser et al.,[26] was cultured in RPMI 1640 Dutch modified medium (Gibco), supplemented with 10% FBS (Greiner Bio-one), 1% GlutaMAX, and 1% Penicillin/Streptomycin (Gibco). To generate CM cells with red fluorescence, cells were stably transduced with lentivirus expressing both tandem dimer (td)Tomato and Blasticidin-S, as previously described[28]. Virus-containing medium was replaced with fresh medium containing Blasticidin-S (2 µg/mL) to select transduced cells. Transduction of the cells with the tdTomato-expressing virus did not alter the growth pattern of parental cells. After transduction, cells were incubated with multiplicity of infection (MOI) of 2.0 in medium with 8.0-µg/mL polybrene for 16 hours. For cultivation of stable transgenic tdTomato-expressing cells, Blasticidin-S (2 µg/mL) was added to the complete medium.

Growth Kinetics of Tomato-Red Cells *In Vitro*

Transgenic tdTomato-expressing cell lines were seeded in triplicate in 96-well plates at a density of 600, 1200, and 2400 for CRMM-1 and CRMM-2 cell lines in a total volume of 100 µL of medium. Because the CM2005.1 cell line is smaller than the others, it was seeded in triplicate in 96-well plates at a density of 1000, 2000, and 4000 cells per well, in a total volume of 100 µL of medium. For testing vemurafenib, cells were seeded at a density of 2000 (CRMM-1 and CRMM-2) or 3500 (CM2005.1) cells per well, in a total volume of 100-µL medium. Cell proliferation was analyzed at 1, 3, and 5 days of incubation by an In-Cell Western assay (Odyssey Infrared Imaging

System, LI-COR, Leusden, The Netherlands): after removing the medium, cells were fixed for 1 hour in 4% formaldehyde and incubated with DRAQ5, a far-red fluorescent DNA dye (1:8000, DR50050; Biostatus Ltd., Loughborough, UK). After washing with 0.1% Tween-PBS buffer, plates were scanned with an Odyssey Infrared Imaging System (LI-COR). Odyssey 3.0 software was used to quantify signal intensity.

Animals and Injection Sites

The (*fli:GFP*) *Casper* transgenic zebrafish[29] were maintained according to standard protocols (http://ZFIN.org, in the public domain) and in compliance with Dutch animal welfare regulations and European Union Animal Protection Directive 2010/63/EU. Our research followed the ARVO Statement for the Use of Animals in Ophthalmic and Vision Research.

When the cells reached 75% to 90% confluency, they were trypsinized (0.05% trypsin-EDTA; Gibco), centrifuged for 4 minutes at 200*g*, washed with Dulbecco's phosphate-buffered saline (DPBS; Invitrogen), and diluted to 250 cells/nL in 2% polyvinylpyrrolidone-40 (PVP-40; Calbiochem, San Diego, CA, USA).

At 2-days postfertilization (dpf), dechorionated zebrafish embryos were injected with this CM cell suspension using glass capillary needles with an opening of approximately 20 to 30 µm. Embryos were anesthetized with 2% tricaine (Sigma-Aldrich Corp., Zwijndrecht, The Netherlands) and positioned in a Petri dish covered with 1% agarose. Using a pneumatic picopump and a manipulator (World Precision Instruments, Sarasota, FL, USA), 200 to 400 cells were injected inside the yolk sac in one group of embryos, or inside the duct of Cuvier in a second group, and 50 to 100 cells were injected around the right eye in a third group of zebrafish. The embryos were each placed individually in a well of a 48-well plate, with 1 mL of egg water (60-µg/mL OceanSalt in demi water) in each well and maintained at 34°C, which was the optimal temperatures for cell growth and zebrafish embryo development[30]. The egg water was refreshed daily and the injected embryos were evaluated at 2-, 4-, and 6-days postinjection (dpi), using a fluorescence stereo microscope (Leica M205FA; Leica Microsystems, Inc., Buffalo Grove, IL, USA).

Kaplan-Meier Survival Analysis of Injected Embryos

After establishing the optimal injection site for CM cells in zebrafish, we determined how injection of cancer cells influenced embryo survival, shown in a Kaplan-Meier survival analysis (cumulative survival curve). Tumor cells were injected into the Duct of Cuvier at 2 dpf. One group (*n* = 90) was injected with CRMM-1, a second group (*n* = 201) with CRMM-2, and the third group (*n* = 221) received an injection with CM2005.1. A fourth group (*n* = 121) received an injection with PVP-40 and the last group (*n* = 96) was not injected. The number of injected cells was between 200 and 400 per embryo. After injection, the embryos were maintained at 34°C, and scored daily for survival, without changing the egg water, until 6 dpi.

Phenotype of CM Cell Lines in Zebrafish and Cell Migration

The embryos were injected with CRMM-1, CRMM-2, or CM2005.1 cells and screened at 1 dpi under the same conditions as described above. Embryos were anaesthetized with 2% tricaine at 1, 4, and 6 dpi to perform image analysis using a fluorescence stereo microscope and a confocal microscope (Leica TCS SPEl; Leica Microsystems, Inc.). For cell growth quantification, the pixel numbers that represent the amount of cells were counted at 1 and 6 dpi, using ImageJ software.[31]

Statistical analysis was performed using R version 2.15.1.[32] The difference in growth among the three cell lines in the embryos was analyzed using a generalized linear model (GLM) with normal distribution after square-root transformation of the data.

Immunohistochemistry (IHC)

After 6 dpi, injected whole embryos were fixed in 4% paraformaldehyde and stored in 100% methanol at −20°C. To perform IHC, embryos were rehydrated, washed with PBS-TX, and permeabilized with 10 µg/mL of protease K in PBS-TX at 37°C (in a water bath) for 10 minutes. Then, they were washed three times using PBS-TX for 10 minutes and put in blocking buffer at room temperature (RT) for 1 hour. Following this, whole embryos were incubated with Ki67 rabbit antibody at a dilution of 1:200 (Abcam, Cambridge, UK), at RT for 2 hours and stored overnight at 4°C. After that, the embryos were washed and incubated with the second antibody, Alexa fluor 633 anti-rabbit at a 1:200 dilution (Invitrogen) at RT for 2 hours and stored overnight at 4°C. The immune-

stained whole embryos were arranged on a microplate and covered with 1% low melting agar to take pictures with a confocal microscope.

Toxicity Test and *in vivo* inhibitor treatment.

For the *in vivo* toxicity test, 1mL of drug-containing egg water was put into the wells of a 24-well plate. Six noninjected 3-dpf zebrafish embryos were placed in each well, maintained at 34°C and observed daily until 8 dpf. The drugs were refreshed every 2 days and all experiments were performed in triplicate. A drug concentration was considered nontoxic when survival was equal or higher than 80%.

At 2 dpf, embryos were injected with CRMM-1, CRMM-2, or CM2005.1 cells and treatment with Vemurafenib was started at 1 dpi. They were treated for 5 days with the inhibitor, changing the egg water and inhibitor twice, and photographed at 1 and 6 dpi using the fluorescence stereo microscope. Using ImageJ software,[31] pixel numbers were determined.

Results

Growth Kinetics of Tomato-Red Cells *In Vitro*

Our goal was to establish a CM xenograft model allowing the *in vivo* screening of drugs. We used tdTomato-red expressing cells to track the proliferation and migration of tumor cells *in vivo*. To verify the possible adverse effect of tdTomato expression on cellular growth kinetics, we used an In-Cell Western proliferation assay. No effect was observed until 5 days of incubation (Supplementary Fig. S1), indicating that we could use the tdTomato overexpressing cells in the zebrafish.

Injection Sites

To establish the model, we tested three different injection sites: engraftment around the eye, in the yolk sack, or in the duct of Cuvier. The duct of Cuvier is the common cardinal vein formed by the left and right posterior cardinal veins joining up with the anterior cardinal vein. The duct of Cuvier functions as an embryonic vein structure collecting all venous blood and leads directly to the heart's sinus venosus; it carries the blood ventrally across the yolk sac.[33] Using this site of injection ensures a rapid and a near complete dissemination of injected cancer cells throughout the blood circulation.[34]

Injecting tumor cells around the eye was technically challenging because of the small size of the eye, limiting throughput and increasing lethality. After injecting tumor cells around the eye, the cells disseminated to the head, inside the eye, and inside the circulation (Figs. 1A, 1B). Injecting cells inside the yolk sac was easy to perform, but after 6 dpi, many cells had died (Figs. 1C, 1D). Injections into the duct of Cuvier were relatively easy to perform and cells survived and proliferated (Figs. 1E, 1F).

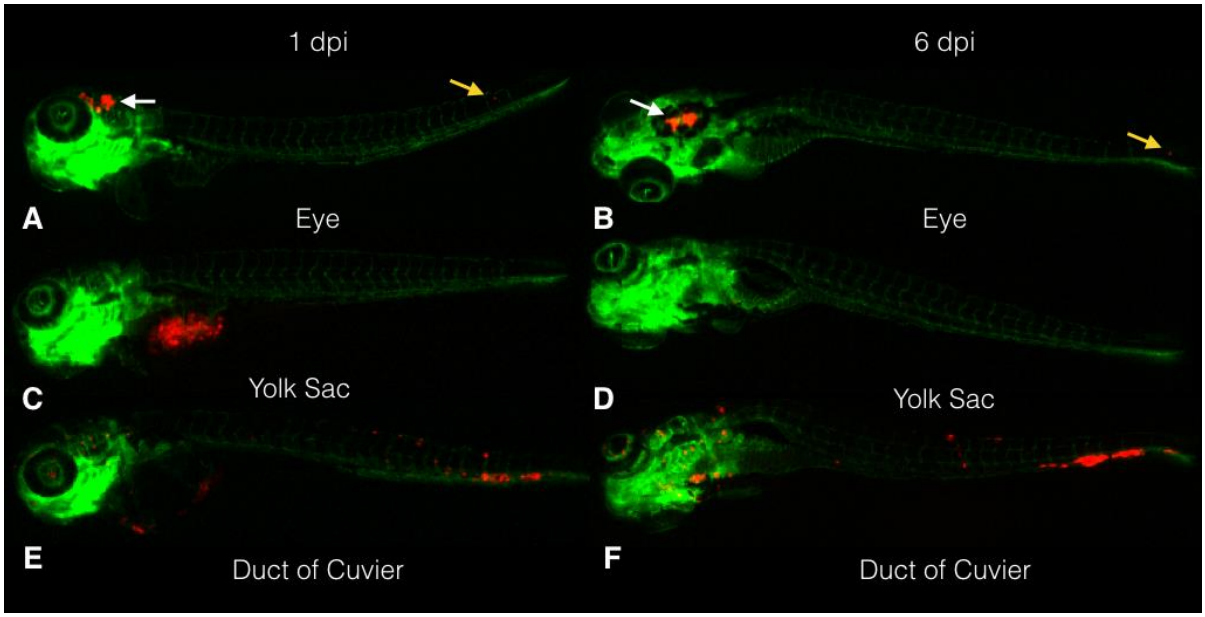

Figure 1. Stereo fluorescence image of zebrafish embryos engrafted with CM cells (vasculature in *green* and CM cells in *red*). The embryos were injected at 2 dpf with CRMM-1 CM cells labeled with tomato-red (*red*). Photographs taken of the same embryo that had been injected with CM cells around the eye at 1 (**A**) and 6 dpi (**B**), showing cells inside the head (*white arrows*) and in the tail (*yellow arrow*). Following injection in the yolk sac, an embryo shows the cells in the yolk sac at 1 (**C**), but not 6 dpi (**D**). After injection of cells into the duct of Cuvier, cells are seen inside the circulation at 1 dpi (**E**), mainly in the tail and inside the eye. The same embryo shows a cluster in the tail and cells inside the eye at 6 dpi (**F**). The stereo fluorescent images (original magnification: ×20) are representative of >10 independent experiments.

The injection into the duct of Cuvier ensures that the cells have access to the endothelium and their intrinsic adhesion molecules and nutrients and helps to disseminate the cells throughout the body. As the duct of Cuvier is the most reliable and biologically relevant injection site, we used this site in all subsequent experiments. The cumulative survival curves of all groups were above 80% (Fig. 2).

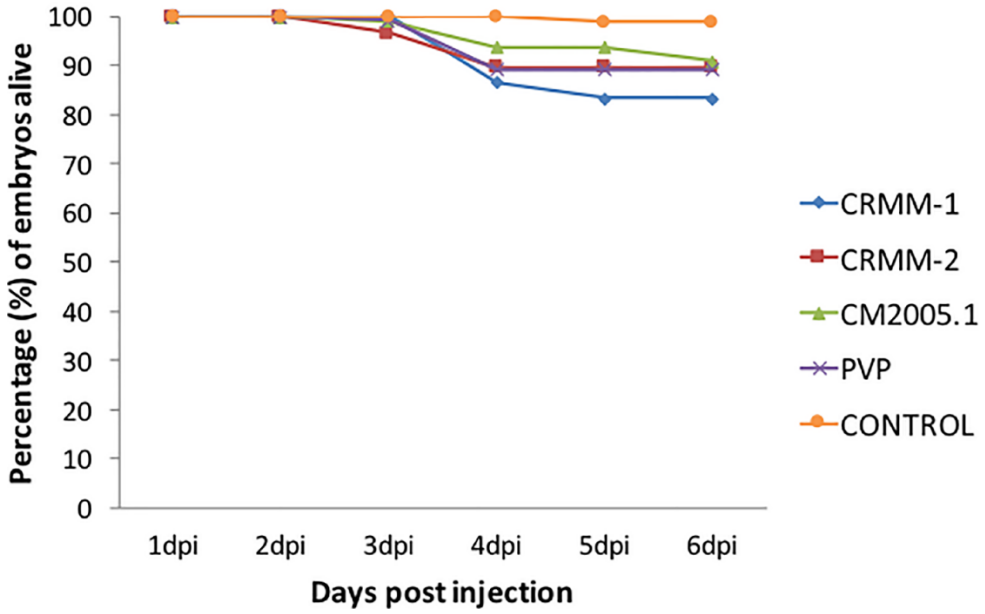

Figure 2. Survival of (*fli:GFP*) *Casper* embryos injected with different types of CM cells, after injection of 200 to 400 cells in the duct of Cuvier on 2 dpf. The number of embryos were: *n*CRMM-1 = 90, *n*CRMM-2 = 201, *n*CM2005.1 = 221, *n*PVP = 121, and *n*Control = 96.

Phenotype of CM Cells in Zebrafish

After cells had been injected inside the duct of Cuvier, migration was assessed. With all three cell lines, 10% to 30% of the embryos had cells inside the eye and between 58% and 64% of embryos showed cells in the tail (Fig. 3). At 1 dpi, cells from all three cell lines had disseminated to the eye and to the tail, forming clusters at 4 and 6 dpi, with more prominent clusters occurring when we used cell line CM2005.1 (Fig. 4). Cells from all three cell lines grew inside, outside, and around vessels during the 6 days of observation (Fig. 4). More tumor cells were observed at 6 dpi than at 1 dpi ($P < 0.001$ for CRMM-1, $P = 0.04$ for CRMM-2, and $P = 0.001$ for CM2005.1) (Fig. 5).

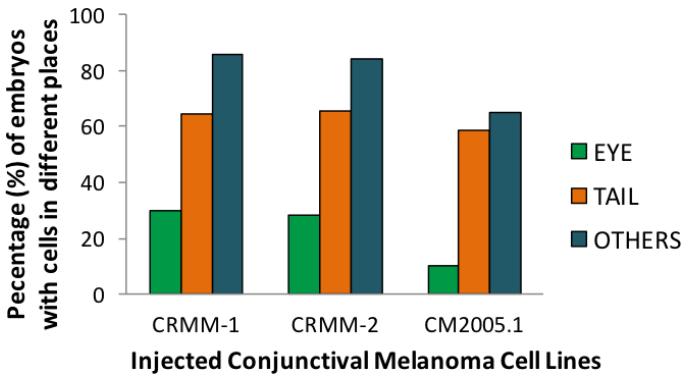

Figure 3. Location of tumor cells at 6 dpi in (*fli:GFP*) *Casper* zebrafish embryos after injection of 200 to 400 cells of the different CM cell lines into the duct of Cuvier at 2 dpf. Tumor cell locations were scored using a stereo fluorescence microscope. The same embryo could harbor cells in more than one place at the same time. "Others" indicates cancer cell retention/outgrowth at the base of the heart or in the head region. The number of embryos used was $n_{CRMM-1} = 70$, $n_{CRMM-2} = 81$, and $n_{CM2005.1} = 77$.

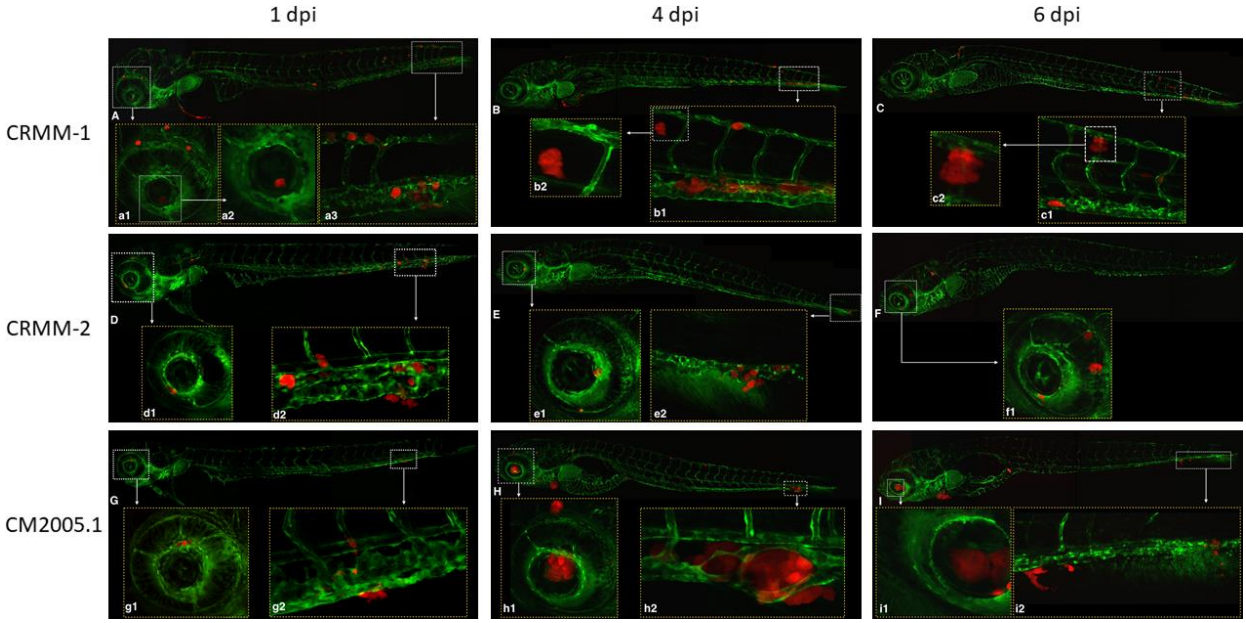

Figure 4 Confocal micrographs of the observed phenotypes at 1, 4, and 6 dpi after engraftment of three CM cell lines via the duct of Cuvier in (*fli:GFP*) *Casper* zebrafish embryos. At 1 dpi, CRMM-1 (A), CRMM-2 (D), and CM2005.1 (G) cells were already inside the eye (a1, a2, d1, g1) and in the tail (a3, d2, g2). At 4 (B, E, H), and 6 dpi (C, F, I), cells formed clusters in the tail and in the eye in all three cell lines (data not shown). The clusters were more evident in the tail (h2) and in the eye (h1, i1) after injection of cell line CM2005.1. The three cell lines (data not show) grew inside (a3, b1, d2, e2, g2, h2, i2), outside (b2), and around (c2) the vessels and the cells could be found inside the eye (f1, i1) until 6 dpi. The images were acquired using a Leica TCS SPE confocal microscope and managed in ImageJ software. Images (A–I) ×10 dry objective. All the other images: ×20 dry objective. *Red*: cells labeled with tdTomato; *green*: GFP-endothelial cells of the (*fli:GFP*) *Casper* lines.

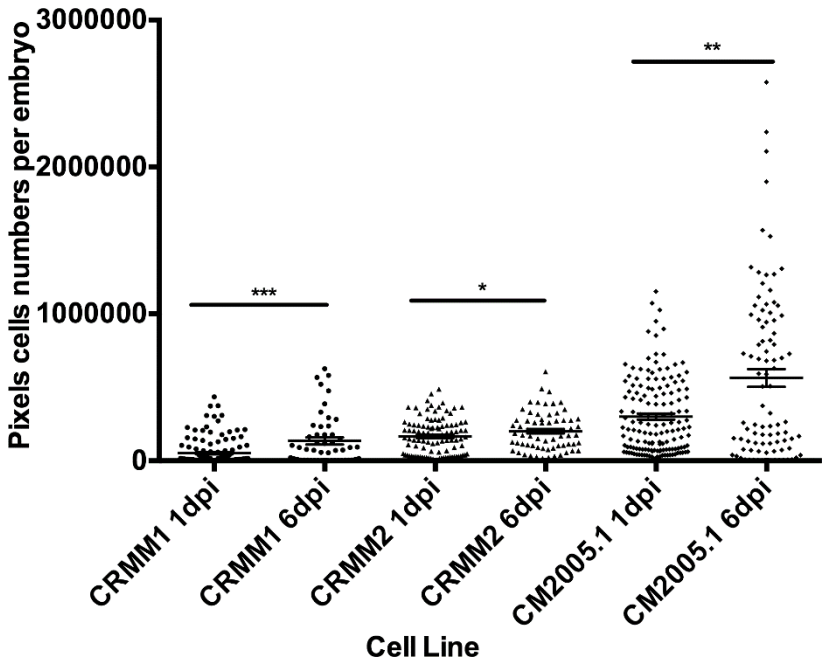

Figure 5. Outgrowth of CM cells *in vivo* in (*fli:GFP*) *Casper* zebrafish embryos engrafted with 200 to 400 cells of CM cell lines at 2 dpf via the duct of Cuvier. Images were taken at 1 and 6 dpi. Each point means one embryo and the pixel number indicates the amount of fluorescence cells counted using ImageJ software. Statistical significances were calculated by general linear model (ANOVA) and *P* values were as follows: **P* < 0.05, ***P* < 0.01, ****P* < 0.001. For all groups: *n* ≥ 51.

Immunohistochemistry (IHC)

As the image analysis suggested that the cells had divided inside the zebrafish, we tested this using IHC with the Ki67 antibody at 6 dpi. Some cells from all three CM cell lines stained positive for Ki67 at 6 dpi and in some cases, mitotic figures in tumor cells were observed (Fig. 6). These findings show that the CM cells proliferated 6 days after injection inside the duct of Cuvier.

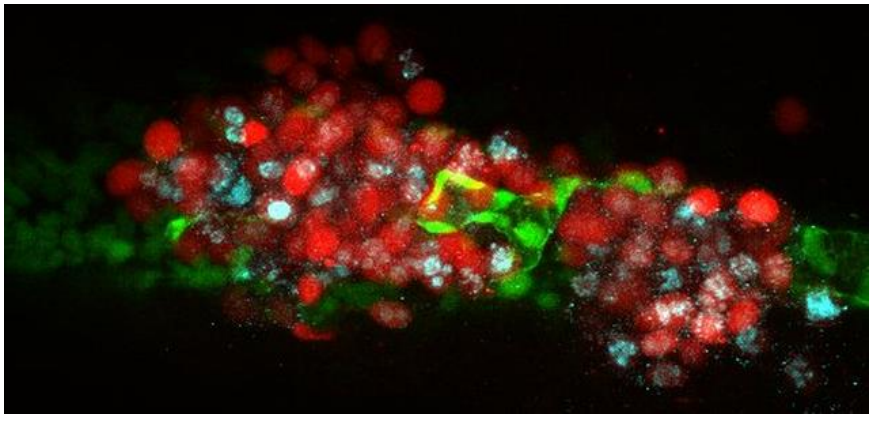

Figure 6. Confocal image of immunohistochemistry with Ki67 in a whole 6 dpi (*fli:GFP*) *Casper* zebrafish embryo. There were 200 to 400 CRMM-1 td-Tomato CM cells injected into the duct of Cuvier. We see tumor cell (*red*) migration outside the vessels (*green*); cell proliferation is indicated by Ki67 staining (*blue*). This image of the tail of a live embryo was acquired by confocal microscope (×20 dry objective). Similar images were obtained from all three CM cell lines in >10 independent experiments.

Toxicity test and treatment with vemurafenib *in vivo*

Vemurafenib inhibits the proliferation of the CM cell lines *in vitro* in a mutation-dependent way (Supplementary Fig. S2) and was, therefore, used to test the *in vivo* model. The toxicity test resulted in 94% survival at 7 and 8 dpf at a concentration of 0.25 μM, and 94% at 8 dpf when the 0.5-μM concentration was used (Supplementary Fig. S3). For all the other tested concentrations, survival of the embryos was 100%. As the drug concentration was considered nontoxic when survival was equal or higher than 80%, we concluded that vemurafenib was nontoxic to the zebrafish at the evaluated concentrations.

Considering that the highest concentrations of vemurafenib that had been evaluated *in vitro* were 3.2 μM (CRMM-1 and CRMM-2) and 0.32 μM (CM2005.1), and that this compound was nontoxic to the embryos up to a concentration of 4.0 μM, we chose a final concentration 4.0 μM/mL to treat engrafted embryos up to 5 dpi because the compound was added in egg water.

At 5-days post treatment with 4 μM of vemurafenib, we noticed inhibition of CRMM-1 (Fig. 7A) and CM2005.1 (Fig. 7C) cell growth when compared with control groups; proliferation of CRMM-2 was not affected by vemurafenib (Fig. 7B; vemurafenib treatment versus control $P = 0.013$ for CRMM-1, $P = 0.007$ for CM2005.1, and $P = 0.33$ for CRMM-2).

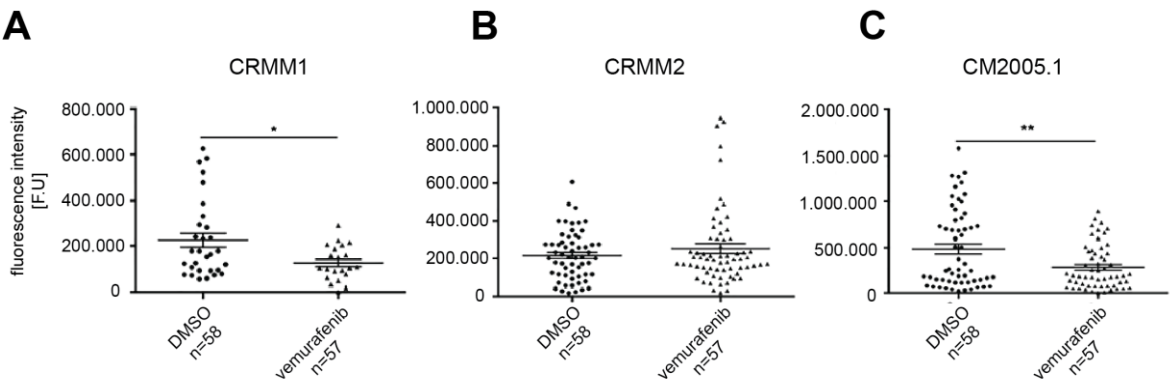

Figure 7. *In vivo* effect of 4-μM Vemurafenib on cell behavior in (*fli:GFP*) *Casper* zebrafish embryos engrafted via the duct of Cuvier with three CM cell lines, determined after 5 days. The images show a decrease in pixel numbers of cell lines CRMM-1 (A) and CM2005.1 (C), but not of CRMM-2 (B). Each point means one embryo and the pixel numbers are the fluorescent pixels counted using ImageJ software. Statistical significances were calculated by general linear model (ANOVA) and *P* values were indicated as follows: **P* < 0.05, ***P* < 0.01.

Discussion

Our results showed that when CM cells were injected around the eye (at 2 dpf), they accidentally passed into the circulation and frequently ended up in the tail, head, and ocular vessels. This is because there is a complex system of retinal blood vessels in the zebrafish's eye and intraocular vessels are already detected at 60-hours postfertilization[35].The vasculature develops quickly and, at 5 dpf, reaches from the optic disk to the intraocular lens. This site of injection is so rich in vessels that it has been used to inject cells into the circulation in adult zebrafish[36].

We believe that the injection in the yolk sac leads to cell death of the many engrafted cells because the yolk sac is a lipid-rich environment devoid of blood circulation and sparse in nutrient and adhesion molecules. Furthermore, some cells that had been injected in the yolk sac passively migrated to the embryo's body (e.g., the tail, the head or inside the eye, directly after engraftment). This may have occurred because the cells were inadvertently introduced inside the circulation, as the duct of Cuvier, the common cardinal vein, crosses the yolk sac and leads directly to the heart's venous sinus[33]. In contrast to Haldi et al.,[30] who recommended that injections can be made anywhere in the yolk sac, we believe that the injections can be done in the yolk sac while avoiding the duct of Cuvier, but we did not use this approach: our experiments show that injecting into the Duct of Cuvier led to the most reproducible results. The model that we used represents a metastatic disease model, as human CM cells were injected into the circulation of the zebrafish embryos[37].

Using Ki67 staining, we showed that CM cells survived and proliferated inside the fish until at least 6 dpi. We furthermore observed that 58% to 64% of all engrafted embryos showed dissemination of the cells to the tail at 6 dpi, demonstrating a preference of all three cell lines for this site. We believe that the reason why these cells ended up in the tail was mainly because of the presence of the caudal hematopoietic tissue (CHT) in this site. Myeloid cells have been detected at the posterior end of the CHT and are

involved in the process of both tumor vascularization and invasion, which are critical steps toward localized tumor growth and micro-metastasis formation[38]. Once the cells have reached the CHT, we believe that they are arrested there through physical entrapment and due to a slower blood flow. The CHT harbors numerous stem cell components driving metastasis formation and proliferation. The zebrafish embryo can be used to study the interaction between the innate immune system (neutrophils and macrophages) and tumor cell behavior: this is one of the reasons why we set out to develop this CM model[37,38].

The mutations involved in CM are more similar to cutaneous melanoma than uveal melanoma. Cutaneous melanoma and CM harbor a *B-RAF* mutation, while in most uveal melanoma, *GNAQ/GNA11* mutations occur[39,40]. While all three cell lines were derived from primary tumors and not from metastases, all of them migrated into the eyes in a considerable proportion of engrafted zebrafish embryos (30% of CRMM-1, 28% of CRMM-2, 10% of CM2005.1). However, metastatic cutaneous human melanoma did not migrate to the eyes when injected into zebrafish embryos[30,41]. In a recent study,[42] primary and metastatic uveal melanoma cells were seen to migrate to the eye in 10% of the embryos. This suggests that the migration of eye cancer cells to the eye is not mutation dependent, but controlled by others factors, which should be evaluated in the future.

We determined whether the CM zebrafish model can be used to test drugs: vemurafenib inhibited the growth of cell lines CRMM-1 and CM2005.1 *in vivo* and *in vitro*, and not of cell line CRMM-2. The results *in vitro* were expected as CRMM-1 and CM2005.1 harbor a *B-RAF V600E* mutation, while the CRMM-2 cell line contains an *N-RAS Q61L* mutation[17,27]. Vemurafenib was approved in 2011 by the Food and Drug Administration for treatment of unresectable melanoma harboring *B-RAF V600E* mutations[43] and is a potent agent for treatment of *B-RAF V600E*-positive melanoma[44]. It has been used to target metastases and a primary CM[45]. Vemurafenib was previously shown to have a selective effect on CM cell lines *in vitro*[46] and we used that information to validate the usability of the zebrafish CM model. In our experiments, the effects of the vemurafenib in the treatment of engrafted embryos were the same as those observed *in vitro* showing that the zebrafish embryo model can be used in drug screens against human CM.

Conclusions

The zebrafish model that we describe here allows migration and proliferation of three human CM cell lines. These cells induced a phenotype that was highly reproducible when injected via the duct of Cuvier. The engrafted embryos tolerated the treatment with vemurafenib well, while this inhibitor affected the cell proliferation *in vivo* in a mutation-dependent manner. Thus, we conclude that the (*fli:GFP*) *Casper* zebrafish embryos can be used as an efficient animal model to study metastatic behavior of CM cells and for preclinical testing of new treatments against human CM.

Acknowledgments

The authors thank Aart G. Jochemsen for transducing the cells with tomato-red.

Supported by grants from the National Council of Technological and Scientific Development CNPq (200746/2015-4; Brasilia, DF, Brazil), and the China Scholarship Council (Beijing, China).

Disclosure: K.C.S. Pontes, None; **A. Groenewoud**, None; **J. Cao**, None; **L.M.S. Ataide**, None; **E. Snaar-Jagalska**, None; **M.J. Jager**, None

References

1. Harooni H, Schoenfield LR, Singh AD. Current appraisal of conjunctival melanocytic tumors: classification and treatment. *Future Oncol*. 2011; 7: 435–446.
2. Tuomaala S, Eskelin S, Tarkkanen A, Kivela T. Population-based assessment of clinical characteristics predicting outcome of conjunctival melanoma in whites. *Invest Ophthalmol Vis Sci*. 2002; 43: 3399–3408.
3. Yu GP, Hu DN, McCormick S, Finger PT. Conjunctival melanoma: is it increasing in the United States? *Am J Ophthalmol*. 2003; 135: 800–806.
4. Triay E, Bergman L, Nilsson B, All-Ericsson C, Seregard S. Time trends in the incidence of conjunctival melanoma in Sweden. *Br J Ophthalmol*. 2009; 93: 1524–1528.
5. Riechardt AI, Maier AB, Nonnenmacher A, et al. B-Raf inhibition in conjunctival melanoma cell lines with PLX 4720. *Br J Ophthalmol*. 2015; 99: 1739–1745.
6. Shields CL, Markowitz JS, Belinsky I, et al. Conjunctival melanoma: outcomes based on tumor origin in 382 consecutive cases. *Ophthalmology*. 2011; 118: 389–395.
7. Errington JA, Conway RM, Walsh-Conway N, et al. Expression of cancer-testis antigens (MAGE-A1, MAGE-A3/6, MAGE-A4, MAGE-C1 and NY-ESO-1) in primary human uveal and conjunctival melanoma. *Br J Ophthalmol*. 2012; 96: 451–458.
8. Jovanovic P, Mihajlovic M, Djordjevic-Jocic J, et al. Ocular melanoma: an overview of the current status. *Int J Clin Exp Pathol*. 2013; 6: 1230–1244.
9. Werschnik C, Lommatzsch PK. Long-term follow-up of patients with conjunctival melanoma. *Am J Clin Oncol*. 2002; 25: 248–55.
10. Missotten GS, Keijser S, De Keizer RJ, De Wolff-Rouendaal D. Conjunctival melanoma in the Netherlands: a nationwide study. *Invest Ophthalmol Vis Sci*. 2005; 46: 75–82.
11. Shildkrot Y, Wilson MW. Conjunctival melanoma: pitfalls and dilemmas in management. *Curr Opin Ophthalmol*. 2010; 21: 380–386.
12. Gear H, Williams H, Kemp EG, et al. B-Raf mutations in conjunctival melanoma. *Invest Ophthalmol Vis Sci*. 2004; 45: 2484–2488.
13. Goldenberg-Cohen N, Cohen Y, Rosenbaum E, et al. T1799 B-Raf mutations in conjunctival melanocytic lesions. *Invest Ophthalmol Vis Sci*. 2005; 46: 3027–3030.
14. Griewank KG, Westekemper H, Schilling B, et al. Conjunctival melanoma harbor BRAF and NRAS mutations-response. *Clin Cancer Res*. 2013; 19: 6331–6332.
15. Satyamoorthy K, Li G, Guerrero MR, Brose MS, et al. Constitutive mitogen-activated protein kinase activation in melanoma is mediated by both BRAF mutations and autocrine growth factor stimulation. *Cancer Res*. 2003; 63: 756–759.
16. Banerji U, Affolter A, Judson I, Marais R, Workman P. BRAF and NRAS mutations in melanoma: potential relationships to clinical response to HSP90 inhibitors. *Mol Cancer Ther*. 2008; 7: 737–739.
17. De Waard NE, Cao J, McGuire SP, et al. A murine model for metastatic conjunctival melanoma. *Invest Ophthalmol Vis Sci*. 2015; 56: 2325–2333.
18. Schlereth SL, Iden S, Mescher M, et al. A novel model of metastatic conjunctival melanoma in immune-competent mice. *Invest Ophthalmol Vis Sci*. 2015; 56: 5965–5973.

19. Konantz M, Balci TB, Hartwig UF, et al. Zebrafish xenografts as a tool for *in vivo* studies on human cancer. *Ann N Y Acad Sci*. 2012; 1266: 124–137.

20. Granato M, Nusslein-Volhard C. Fishing for genes controlling development. *Curr Opin Genet Dev*. 1996; 6: 461–468.

21. Chen JN, Fishman MC. Zebrafish tinman homolog demarcates the heart field and initiates myocardial differentiation. *Development*. 1996; 122: 3809–3816.

22. Tulotta C, Stefanescu C, Beletkaia E, et al. Inhibition of signaling between human CXCR4 and zebrafish ligands by the small molecule IT1t impairs the formation of triple-negative breast cancer early metastases in a zebrafish xenograft model. *Dis Model Mech*. 2016; 9: 141–153.

23. Stoletov K, Montel V, Lester RD, Gonias SL, Klemke R. High-resolution imaging of the dynamic tumor cell vascular interface in transparent zebrafish. *Proc Natl Acad Sci U S A*. 2007; 104: 17406–17411.

24. White RM, Sessa A, Burke C, et al. Transparent adult zebrafish as a tool for *in vivo* transplantation analysis. *Cell Stem Cell*. 2008; 2: 183–189.

25. Nareyeck G, Wuestemeyer H, von der Haar D, Anastassiou G. Establishment of two cell lines derived from conjunctival melanomas. *Exp Eye Res*. 2005; 81: 361–362.

26. Keijser S, Maat W, Missotten GS, De Keizer RJ. A new cell line from a recurrent conjunctival melanoma. *Br J Ophthalmol*. 2007; 91: 1566–1567.

27. De Waard NE, Kolovou PE, McGuire SP, et al. Expression of multidrug resistance transporter ABCB5 in a murine model of human conjunctival melanoma. *Ocul Oncol Pathol*. 2015; 1: 182–189.

28. Carlotti F, Bazuine M, Kekarainen T, et al. Lentiviral vectors efficiently transduce quiescent mature 3T3-L1 adipocytes. *Mol Ther*. 2004; 9: 209–17.

29. Lawson ND, Weinstein BM. *In vivo* imaging of embryonic vascular development using transgenic zebrafish. *Dev Biol*. 2002; 248: 307–318.

30. Haldi M, Ton C, Seng WL, McGrath P. Human melanoma cells transplanted into zebrafish proliferate, migrate, produce melanin, form masses and stimulate angiogenesis in zebrafish. *Angiogenesis*. 2006; 9: 139–151.

31. Schindelin J, Arganda-Carreras I, Frise E, et al. Fiji: an open-source platform for biological-image analysis. *Nat Methods*. 2012; 9: 676–682.

32. R Development Core Team. *R: A Language and Environment for Statistical Computing*. Vienna: R Foundation for Statistical Computing; 2012.

33. Kimmel CB, Ballard WW, Kimmel SR, Ullmann B, Schilling TF. Stages of embryonic development of the zebrafish. *Dev Dyn*. 1995; 203: 253–310.

34. Helker CSM, Schuermann A, Karpanen T, et al. The zebrafish common cardinal veins develop by a novel mechanism: lumen ensheathment. *Development*. 2013; 140: 2776–2786.

35. Alvarez Y, Cederlund M, Cottell D, et al. Genetic determinants of hyaloid and retinal vasculature in zebrafish. *BMC Dev Biol*. 2007; 7: 114.

36. Pugach EK, Li P, White R, Zon L. Retro-orbital injection in adult zebrafish. *J Vis Exp*. 2009; (34): e1645.

37. Feng Y, Martin P. Imaging innate immune responses at tumour initiation: new insights from fish and flies. *Nature Rev Cancer*. 2015; 15: 556–562.

38. He S, Lamers GEM, Beenakker JM, et al. Neutrophil-mediated experimental metastasis is enhanced by VEGFR inhibition in a zebrafish xenograft model. *J Pathol*. 2012; 227: 431–445.

39. Sendlove HE, Damato BE, Humphreys J, Barker KT, Hiscott PS, Houlston RS. BRAF mutations are detectable in conjunctival but not uveal melanomas. *Melanoma Res*. 2004; 14: 449–452.

40. Van Raamsdonk CD, Griewank KG, Crosby MB, et al. Mutations in GNA11 in uveal melanoma. *N Engl J Med*. 2010; 363: 2191–2199.

41. Lee LMJ, Seftor EA, Bonde G, Cornell RA, Hendrix MJ. The fate of human malignant melanoma cells transplanted into zebrafish embryos: Assessment of migration and cell division in the absence of tumor formation. *Dev Dyn*. 2005; 233: 1560–1570.

42. Van Der Ent W, Burrello C, Lange MJ, et al. Embryonic zebrafish: different phenotypes after injection of human uveal melanoma cells. *Ocul Oncol Pathol*. 2015; 1: 170–181.

43. Bollag G, Tsai J, Zhang J, et al. Vemurafenib: the first drug approved for BRAF-mutant cancer. *Nat Rev Drug Discov*. 2012; 11: 873–886.

44. Flaherty KT, Puzanov I, Kim KB, et al. Inhibition of mutated, activated BRAF in metastatic melanoma. *N Engl J Med*. 2010; 363: 809–819.

45. Pahlitzsch M, Bertelmann E, Mai C. Conjunctival melanoma and BRAF inhibitor therapy. *J Clin Exp Ophthalmol*. 2014; 5: 322.

46. Cao J, Renier C, Aart G, et al. Targeting of the MAPK and AKT pathways in conjunctival melanoma shows potential synergy. *Oncotarget*. 2016; 8: 58021–58036.